AFRL-RD-PS-
TP-2009-1014

AFRL-RD-PS
TP-2009-1014

MISREGISTRATION IN ADAPTIVE OPTICS SYSTEMS: POST PRINT

Nathan D. Engstrom
Jason D. Schmidt

01 June 2009

Technical Paper

AIR FORCE RESEARCH LABORATORY
Directed Energy Directorate
3550 Aberdeen Ave SE
AIR FORCE MATERIEL COMMAND
KIRTLAND AIR FORCE BASE, NM 87117-5776

REPORT DOCUMENTATION PAGE

Form Approved
OMB No. 0704-0188

1. REPORT DATE *(DD-MM-YYYY)*	**2. REPORT TYPE**	**3. DATES COVERED** *(From - To)*
01/06/2009	Technical Paper	June 1, 2009

Misregistration In Adaptive Optics Systems: Post Print

5a. CONTRACT NUMBER
N/A

5b. GRANT NUMBER
N/A

5c. PROGRAM ELEMENT NUMBER
N/A

6. AUTHOR(S)
Nathan D. Engstrom; *Jason D. Schmidt

5d. PROJECT NUMBER
N/A

5e. TASK NUMBER
N/A

5f. WORK UNIT NUMBER
N/A

7. PERFORMING ORGANIZATION NAME(S) AND ADDRESS(ES)

Air Force Research Laboratory
3550 Aberdeen Ave SE
Kirtland AFB, NM 87117

*Air Force Institute of Technology
2950 Hobson Way
Wright-Patterson AFB, Ohio

8. PERFORMING ORGANIZATION REPORT NUMBER

9. SPONSORING / MONITORING AGENCY NAME(S) AND ADDRESS(ES)
Air Force Research Laboratory
3550 Aberdeen Ave SE
Kirtland AFB, NM 87117-5776

10. SPONSOR/MONITOR'S ACRONYM(S)
AFRL/RDSA

11. SPONSOR/MONITOR'S REPORT NUMBER(S)
AFRL-RD-PS-TP-2009-1014

12. DISTRIBUTION / AVAILABILITY STATEMENT
Approved For Public Release

13. SUPPLEMENTARY NOTES
Accepted for Publication in The Optics and Photonics SPIE Proceedings; San Diego, California; August 6, 2009. Public Release Approval 377ABW-2009-0833, 01 Jul 2009. "Government Purpose Rights"

14. ABSTRACT

An adaptive optics (AO) system is most effective when there is a know alignment between the wave front sensor (WFS) and the deformabable mirror (DM). Misregistration is the term for the unknown alignment between the WFS and DM. Misregistration degrades system performance and can make the system unstable. An AO system uses a reconstruction matrix that to transform WFS measurements into dm commands. A standard AO system uses a model reconstruction matrix that assumes perfect registration between the WFS and DM. The object of this research is to mitigate the negative effects of misregistration by using offline WFS measurements to create the reconstruction matrix. To build the reconstruction matrix, each actuator on the dm is poked to a fixed amount, and then the resulting measurement on the WFS is recorded. Analytic studies of the model and measured matrices show that the measured matrix yields a more stable AO system. Additional simulations indicate that applying the measured matrix improves the overall system performance compared to that of the model reconstruction matrix.

15. SUBJECT TERMS
Adaptive Optics; Misregistration; Shack-Hartmann WFS; Self-Referencing Interferometer WFS

16. SECURITY CLASSIFICATION OF:			**17. LIMITATION OF ABSTRACT**	**18. NUMBER OF PAGES**	**19a. NAME OF RESPONSIBLE PERSON**
a. REPORT	**b. ABSTRACT**	**c. THIS PAGE**			Nathan Engstrom
Unclassified	Unclassified	Unclassified	SAR	16	**19b. TELEPHONE NUMBER** *(include area code)* 505-853-3496

Misregistration in Adaptive Optics Systems

Nathan D. Engstrom[a] and Jason D Schmidt[b]

[a]Air Force Research Laboratory, 3550 Aberdeen Ave SE, Kirtland Air Force Base, USA;
[b]Air Force Institute of Technology, 2950 Hobson Way, Wright-Patterson Air Force Base, USA

ABSTRACT

An adaptive optics (AO) system is most effective when there is a known alignment between the wave front sensor (WFS) and the deformable mirror (DM). Misregistration is the term for the unknown alignment between the WFS and DM. Misregistration degrades system performance and can make the system unstable. An AO system uses a reconstruction matrix to transform WFS measurements into DM commands. A standard AO system uses a model reconstruction matrix that assumes perfect registration between the WFS and DM. The object of this research is to mitigate the negative effects of misregistration by using offline WFS measurements to create the reconstruction matrix. To build the reconstruction matrix, each actuator on the DM is poked to a fixed amount, and then the resulting measurement on the WFS is recorded. Analytic studies of the model and measured matrices show that the measured matrix yields a more stable AO system. Additional simulations indicate that applying the measured matrix improves the overall system performance compared to that of the model reconstruction matrix.

Keywords: adaptive optics, misregistration, Shack-Hartmann WFS, self-referencing interferometer WFS

1. INTRODUCTION

Setting up and maintaining a known, fixed optical alignment between an adaptive optics (AO) system's wavefront sensor (WFS) and deformable mirror (DM) is difficult. When the alignment between the WFS and DM is unknown or evolving, the AO system is said to have misregistration. Such misregistration degrades AO performance, and in some conditions, causes instability. Unfortunately, all AO systems have some degree of misregistration, even if it is small. Because of drift in optomechanical mounts and laboratory vibrations, minimizing misregistration requires highly trained engineers to constantly realign the system.

This research focused on developing new mitigation strategies to reduce the negative effects of misregistration using techniques which require less training and more efficient set up procedures for the AO system. The research objectives are to analyze misregistration within AO systems and to investigate mitigation strategies. This research focused only on simple translational misregistration of the DM to the WFS. Translational misregistration is the lateral shift from the nominal position as illustrated in Fig. 1. The main mitigation strategy is to design a new reconstruction matrix for the misaligned system by using the information measured by the WFS. The reconstruction matrix was tested for both the Shack-Hartmann (SH) WFS and the self-referencing interferometer (SRI) WFS in numerical simulations. To further develop current techniques and new designs of building reconstruction matrices, analytical studies and simulations enable understanding of the AO system's stability.

This research used the so-called "poke" method to develop a reconstruction matrix that would be less sensitive to misregistration than an analytic reconstruction matrix. The poke method uses direct WFS measurements to build the reconstruction matrix. This was done by commanding each DM actuator to a fixed level and using the recorded WFS measurement to build the reconstruction matrix. In contrast, the traditional method is to analytically create the matrix from a simple model.

Further author information: (Send correspondence to N.D.E.)
N.D.E.: E-mail: nathan.engstrom@kirtland.af.mil, Telephone: (505) 853-3496
J.D.S.: E-mail: jason.schmidt@ afit.edu, Telephone: (937) 2553636, ext 7224

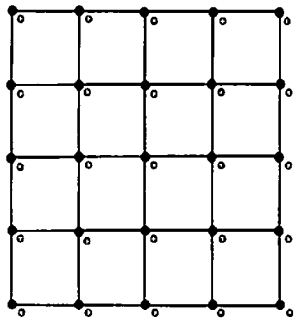

Figure 1. The squares represent the SH WFS subapertures. The dark spots represent nominal actuator positions, and the gray spots are actuators misregistered with respect to the subapertures.

2. ADAPTIVE OPTICS

AO is a class of technologies that compensate for the phase distortion introduced by the atmosphere in real time. The AO system seeks to flatten the phase to provide compensation for phase distortion.[1] The phase distortion that is introduced can be quantified by a few different parameters. The relevant parameters to this research are the Fried parameter and the Greenwood frequency.

The atmospheric coherence width, or Fried parameter, indicates the spatial scale of turbulence at a particular location. This parameter indicates the largest telescope diameter at which resolution no longer improves and is given by[2]

$$r_0 = \left[0.423k^2 \sec\zeta \int_0^L C_n^2(z)dz\right]^{-3/5} \tag{1}$$

for a plane wave, where $k = 2\pi/\lambda$, C_n^2 is integrated over the entire propagation path coordinate z, and L is the propagation distance. Typical values of r_0 are 5-10 cm for a ground-based telescope at sea level observing visible light directly overhead.

The characteristic temporal correlation interval of the atmosphere, called the Greenwood time constant τ_0, is used to identify the interval over which turbulence remains statistically well correlated. The closely related Greenwood frequency is given by

$$f_G = \frac{1}{\tau_0} = \left[2.91k^2 \int_0^L C_n^2(z)V_\perp^{5/3}(z)dz\right]^{3/5}, \tag{2}$$

where $V_\perp(z)$ is the transverse wind velocity as a function of propagation distance.[2] For a constant wind speed $V_\perp$, f_G can be directly related to Fried's parameter by

$$f_G = 0.436\frac{V_\perp}{r_0}. \tag{3}$$

The Greenwood frequency is normally in the range of 20 to 200 Hz.

2.1 DM Control

This research focused on a continuous DM which is constructed on one thin reflective sheet that is attached to the actuators. This coupling of actuators introduces an influence function between neighboring actuators. The

actuator influence function $\mathcal{A}_{kl}$, is the phase caused by poking an individual actuator. It is assumed that $\mathcal{A}_{kl} = 1$ at the location (k, l). The influence function is given by

$$\mathcal{A}(x,y) = \begin{cases} 0 & , \text{ if } |x| > 1 \text{ or } |y| > 1, \\ 1 - |x| & , \text{ if } |y| \leq |x|, \\ 1 - |y| & , \text{ if } |x| \leq |y|. \end{cases} \tag{4}$$

Using the model $\mathcal{A}(x, y)$ set up the geometry matrix Γ, which maps a vector of actuator commands to a vector of subaperture measurements.[3] The AO system is operated in a closed feedback loop with an integral control law. The actuator state integrator is given by

$$\boldsymbol{p}[k+1] = a\boldsymbol{p}[k] + \boldsymbol{u}[k], \tag{5}$$

where $\boldsymbol{p}[k]$ is the current command given to the DM and k is the discrete sample time. The damping factor a is very close to one. Previous sensor measurements are used to build the control vector, $\boldsymbol{u}[k]$. The error, error estimate, and control law are defined by

$$\boldsymbol{e}[k] = \boldsymbol{\phi}[k] - \boldsymbol{p}[k] \tag{6}$$

$$\hat{\boldsymbol{e}}[k] = H\Gamma\boldsymbol{e}[k] \tag{7}$$

$$\boldsymbol{u}[k] = b\hat{\boldsymbol{e}}[k], \tag{8}$$

where b, is the constant control law parameter. The error $\boldsymbol{e}$ is the difference between the aberrated phase of the field, $\boldsymbol{\phi}$, and the phase imparted by the DM, $\boldsymbol{p}$. The error estimate $\hat{\boldsymbol{e}}$ is the result of sensing the gradient of the error which is expressed by Γ and reconstructing the error with H. The control gains are applied to the sequence of error estimates to produce the actuator command vector.[3]

2.2 Reconstruction

As mentioned above, this research used both a SH WFS and a SRI WFS. The SH WFSs are the most commonly used WFS in traditional AO systems. The SH WFS directly measures the gradients of the wavefront and then transforms those measurement into phase using wavefront reconstruction. For this research, the SH WFS used Fried geometry for wavefront reconstruction. In contrast with the Shack-Hartmann WFS, which measures the gradients, the SRI WFS directly measures the wavefront. The SRI WFS is based on a phase-shifting, point diffraction interferometer.[4] The SRI uses the Hudgin reconstruction geometry.

One strategy that has been developed to mitigate the effect of misregistration has been spatial filtering techniques, which attenuates high-frequency content. Each DM geometry has its own set of orthogonal modes (surface shapes). Often, these modes are plagued by a high-frequency rippling, called local waffle. The mechanism for instability is the loss of phase margin in high-frequency modes. This suggests the idea that attenuating the high-frequency spatial response would reduce the stability sensitivity to misregistration.[5] Two specific two-dimensional spatial convolution filters have been developed, the T-filter

$$T = \frac{1}{2}\begin{bmatrix} 0 & \frac{1}{4} & 0 \\ \frac{1}{4} & 1 & \frac{1}{4} \\ 0 & \frac{1}{4} & 0 \end{bmatrix}, \tag{9}$$

and the W-filter

$$W = \frac{1}{4}\begin{bmatrix} \frac{1}{4} & \frac{1}{2} & \frac{1}{4} \\ \frac{1}{2} & 1 & \frac{1}{2} \\ \frac{1}{4} & \frac{1}{2} & \frac{1}{4} \end{bmatrix}. \tag{10}$$

These filters are applied by convolving them with the reconstructed phase. As shown in Fig. 2, SH WFS modes are plagued by local waffle when the least-squares reconstructor is used. For the SRI WFS, an assortment of these modes can be seen in Fig. 3. There is very little local waffle in these modes. This leads to the hypothesis that the SRI provides a more stable system and less sensitivity to translational misregistration.

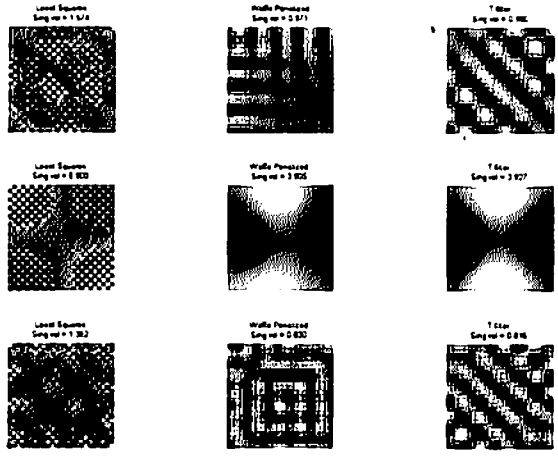

Figure 2. An assortment of three SH modes shows the local waffle in the least-squares reconstructor. Both the waffle-penalized reconstructor and the T-filter reconstructor remove the local waffle. Local waffle increases the instability of the system.

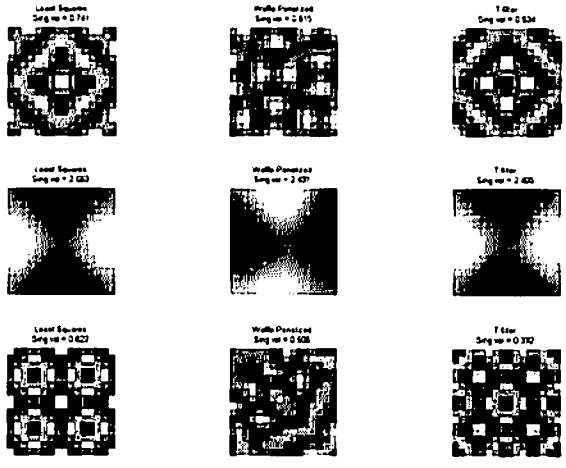

Figure 3. An assortment of three SRI modes shows the local waffle in the least-squares reconstructor. Both the waffle-penalized reconstructor and the T-filter reconstructor remove the local waffle. Local waffle increases the instability of the system.

3. STABILITY TESTING

Several tests were conducted to check AO system stability. The stability tests of the system used the closed-loop poles of the transfer function. In order to find the transfer function, the state space equations needed to be computed. The first-order state space equations for the AO system can be written as

$$\begin{pmatrix} \boldsymbol{p}[k+1] \\ \boldsymbol{p}[k] \end{pmatrix} = \begin{pmatrix} aI - B & 0 \\ I & 0 \end{pmatrix} \begin{pmatrix} \boldsymbol{p}[k] \\ \boldsymbol{p}[k-1] \end{pmatrix} + \begin{pmatrix} B & 0 \\ 0 & 0 \end{pmatrix} \begin{pmatrix} \boldsymbol{\phi}[k] \\ \boldsymbol{\phi}[k-1] \end{pmatrix}, \tag{11}$$

where I and 0 are the identity and zero matrices of the appropriate size. Equation (11) uses the notation

$$B = bH\Gamma \tag{12}$$

and substituting Eqs. (6) to (8) into Eq. (5). The stability of Eq. (11) is due to the eigenvalue locations of the closed-loop matrix

$$A = \begin{pmatrix} aI - B & 0 \\ I & 0 \end{pmatrix}. \tag{13}$$

To state that the system is stable, all the eigenvalues of A need to lie within the unit circle of the complex plane. Finding the numerical eigenvalues of A can be extremely time consuming due to the size of the matrix A. If there are n eigenvalues in $\Lambda(H\Gamma)$, where the operator $\Lambda(\cdot)$ indicates the eigenvalues of a matrix, this equation gives n simple independent equations. Now, for a given set of gains a and b, the closed-loop system is stable if and only if for each $\lambda \in \Lambda(H\Gamma)$ the solutions of

$$\mu^3 - (aI - b\lambda)\mu^2 = 0 \tag{14}$$

all have magnitudes less than unity.[3] This can be called the characteristic equation for stability.

Tests were used to determine the stability of the AO system. A contour plot was developed showing the coupled effects of varying gain and misregistration. Also, the phase margins of the open-loop transfer function were calculated.

3.1 Gain and Misregistration

For the simple integrator, the varying of b has been shown to affect the stability of the system. Examining the closed-loop poles' values as a function of servo gain b and misregistration δ can reveal whether or not a reconstructor H can improve system stability. The set of closed-loop poles for this system are[3]

$$a - b\Lambda(H\Gamma(\delta,\delta)) = \{a - b\lambda : \lambda \in \Lambda(H\Gamma(\delta,\delta)\}. \tag{15}$$

The magnitude of the largest closed-loop pole of a misregistered system with a set δ, a, and b is given by

$$\mathcal{M}(\delta,a,b) = \max(|a - b\Lambda(H\Gamma(\delta,\delta))|). \tag{16}$$

Using this equation, the unity contour line of the system can be plotted. The contour line shows which combinations of gain and misregistration can be on the system without affecting stability. This plot is shown later in Fig. 4.

For this research the measured matrix $\hat{\Gamma}$, which is the true mapping of actuators to sensors, was used instead of the ideal Γ matrix. The contour line of the SH system was calculated for both the WaveProp-generated $\hat{\Gamma}$ and the measured $\hat{\Gamma}$. Where WaveProp is a optical toolbox in Matlab software. To build the contour, the system was misregistered between 0% to 50% of a subaperture. There were 20 misregistration steps in the plot. At each misregistration step, there were 50 steps of gain between 0 to 1. Then Eq. (16) was used to find the unity contour line. Later in Fig. 7 the stability line for the SRI is compared to both stability lines of the SH. The next stability calculation involved the phase margins of the system, as well as other mitigation phase margins.

3.2 Stability Margins

Before instability is reached, the system's performance and stability margins may decrease. This decrease is tracked by examining the phase margins of the system. The phase margins only tracks the stability of the system and not performance. The open-loop transfer function is used to discover how misregistration affects the stability margins. The open-loop transfer function is found by combining Eqs. (5), (7) and (8) to give

$$\boldsymbol{p}[k+1] = a\boldsymbol{p}[k] + bH\Gamma\boldsymbol{e}[k]. \tag{17}$$

Then using the matrix D to diagonalize the equation

$$q_\lambda[k+1] \;\; = \;\; aq_\lambda[k] + b\lambda f_\lambda[k], \tag{18}$$

where

$$\boldsymbol{q} = D^{-1}\boldsymbol{p} \tag{19}$$

$$\boldsymbol{f} = D^{-1}\boldsymbol{e}\,. \tag{20}$$

Because the equation has been diagonalized, Eq. (18) is a system of n independent single-input, single-output equations, one for each eigenvalue of $H\Gamma$. Equation (18) has been simplified using $\boldsymbol{q} = [q_\lambda]$ with λ being the eigenvalues of the matrix $H\Gamma$. Equation (18) can be simplified to

$$q_\lambda[k+1] = aq_\lambda[k] + b\lambda f_\lambda[k-n]. \tag{21}$$

For each of the n equations, the transfer function in the z-domain is analyzed to get the gain and phase margin. The transfer function in the z-domain of Eq. (21) is[5]

$$T_\lambda(z^{-1}) = \lambda\frac{bz^{-n}}{1-az^{-1}}\,. \tag{22}$$

The gain and phase margins for the system are the minimum gain and phase margins of the eigenvalues. If $g_m(\lambda)$ and $p_m(\lambda)$ are the gain and phase margins for the mode corresponding to eigenvalue λ, the the system gain and phase margins are defined by[3]

$$\begin{aligned} G_M &= \min\{g_m(\lambda) : \lambda \in \Lambda(H\Gamma)\} \\ P_M &= \min\{p_m(\lambda) : \lambda \in \Lambda(H\Gamma)\}\,. \end{aligned} \tag{23}$$

With the analytical calculations completed the next step was to build simulations to see how misregistration affects the performance of the AO system.

4. SIMULATION AND TESTING

In order to understand misregistration better, a set of simulations was performed, and the measured Strehl ratios were used to judge AO system performance. The source was assumed to be very far away so that the incoming field could be modeled as a plane wave, an electromagnetic field represented on a grid with 256×256 samples over the field. The source field was passed through a phase screen, thereby adding the distortion due to the atmosphere. The phase screen has specific characteristics to indicate how much phase distortion is added and how quickly the screen is moving. The strength of the distortion is indicated by the Fried parameter $r_0 = 37.5$cm. This value of r_0 was chosen in order to have the ratio of $d/r_0 = 0.5$, where d is the diameter of one subaperture of the WFS.

The phase screen also has a sampling of 256×256 and laterally translates at different velocities for each simulation. The velocity at which the phase screen moves is directly related to the Greenwood frequency of the turbulence according to Eq. (3). The metric used to calculate the velocity of the phase screen was a ratio of the 3-dB bandwidth of the system over Greenwood frequency. For each set-up, the simulation ran with $f_{3dB}/f_G = 5,\ 15$.

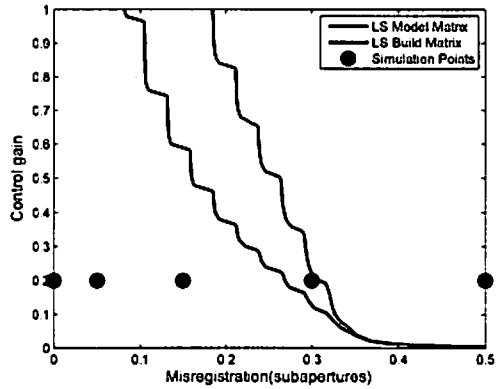

Figure 4. Stability lines of a 15 × 15 subaperture system. This figure illustrates the relationship of instability with misregistration and gain. The area under the curves is the stable region, while the area above the curves is the unstable region. The least-squares model matrix refers to a WaveProp build reconstruction matrix, the least-squares build matrix refers to poke build SH reconstruction matrix.

After the field passed through the phase screen, it was reflected off the DM. The DM was set up to minimize the residual error sensed by the WFS. The DM used in the simulations was set up to be a square mirror without any actuator slaving. The DM was a continuous facesheet DM. The DM had 256 actuators arranged in a 16 × 16 square. Once the field was reflected off the DM, the Strehl ratio was calculated. The field estimated Strehl ratio used in these simulations is given by

$$SR = \frac{|\sum U|^2}{\sum |U|^2}, \tag{24}$$

where U is the compensated optical field. The field was then measured by the WFS and commands were given to the DM for the next time step.

These simulations were conducted using the SH WFS and the SRI WFS separately. The SH WFS has a more fully developed model, and WaveProp has tools to compute a misregistered Γ matrix.

4.1 Shack-Hartmann WFS

Analytical calculations were completed on a general setup for a SH WFS using the Fried geometry. Two analytical calculations were completed, and the stability of the system identified. A simulation was set up using the SH WFS with and a 15 × 15 subaperture system. Different levels of misregistration and different f_{3dB}/f_G levels were tested on the system.

4.1.1 Analytical Calculations

The first analytical calculations were for the SH reconstructor matrix. The first test examines the coupling effects of gain and misregistration. In Fig. 4 phase-margin contours have been drawn. The graph shows that when the combination of gain and misregistration are below the curve, the system is stable. This indicates that the built reconstruction matrix (the red curve) has a greater area of stability than the model matrix(the blue curve). The circles show the different misregistrations that were used in the simulations. The final analytical result is displayed in Fig. 5. This graph shows that the measured reconstructor has better phase margins with misregistration than the model, but not as good as the T- and W-filters.

4.1.2 Results

In Fig. 6 the 15 × 15 subaperture system has a constant general performance, with Strehl ratios in the region between 0.5 and 0.7 on average. The only Strehl ratios to fall out of this region are for the LS model matrix reconstructor in plots (b) and (d). These two graphs are of the systems with the greater misregistration on

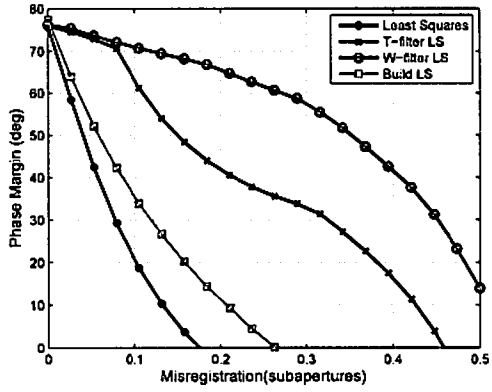

Figure 5. Phase margins of a 15 × 15 subaperture system. This figure illustrates the phase margins that were calculated for misregistration up to half of a subaperture. The model least-squares reconstructor was evaluated as well as the build least-squares reconstructor and the T- and W- filters.

Table 1. SH WFS Strehl ratio averages for a 15 × 15 subaperture system

f_{3dB}/f_G	Misregistration %	Build Matrix Strehl Ratio	Model Matrix Strehl Ratio	% Change
5	0%	0.66	0.65	0.29%
	5%	0.65	0.65	0.4%
	15%	0.63	0.61	3.0%
	30%	0.58	0.19	214.4%
	50%	0.41	0.01	5547.2%
15	0%	0.64	0.64	0.11%
	5%	0.63	0.63	-0.05%
	15%	0.62	0.61	1.0%
	30%	0.58	0.27	114.5%
	50%	0.35	0.01	5461.9%

them. This result is not too surprising as these points do fall around the edge of the stability region found in the analytical calculations. Detailed results of the simulation can be found in Table 1. The table outlines the average Strehl ratio for each scenario. The table shows that the system has its best performances with low misregistration.

4.2 Self-Referencing Interferometer WFS

Analytical calculations were completed on a general setup for a SRI WFS using a Hudgin-based reconstructor to unwrap the phase. Two analytical calculations were completed, and the stability of the system identified. A simulation was set up using the SRI WFS with and a 15×15 subaperture system. Different levels of misregistration and different f_{3dB}/f_G levels were tested on the system.

4.2.1 Analytical Calculations

The first test probes the coupling effects of gain and misregistration. In Fig. 7 a phase-margin contour has been drawn. The graph shows that when the combination of gain and misregistration is at a point below the curve, the system is stable. This graph also shows that the SH built reconstruction matrix (the red curve) has a greater area of stability than the SH model matrix (the blue curve). However, both fall below the SRI built reconstruction (the black curve). This suggests that the SRI should be less sensitive to misregistration than the SH WFS. A comparison to the SRI model matrix was not completed due to the fact that WaveProp does not have a model misregistered matrix for the SRI.

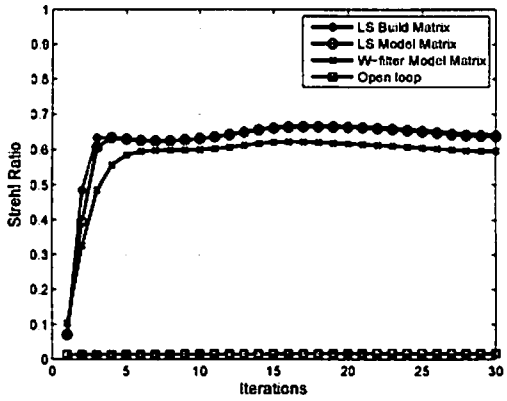

(a) Misregistration = 5%, $f_{3dB}/f_G = 5$

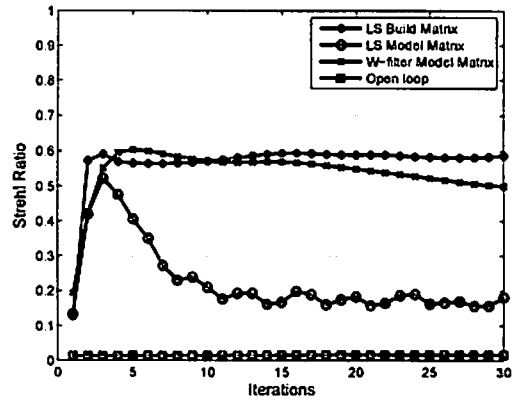

(b) Misregistration = 30%, $f_{3dB}/f_G = 5$

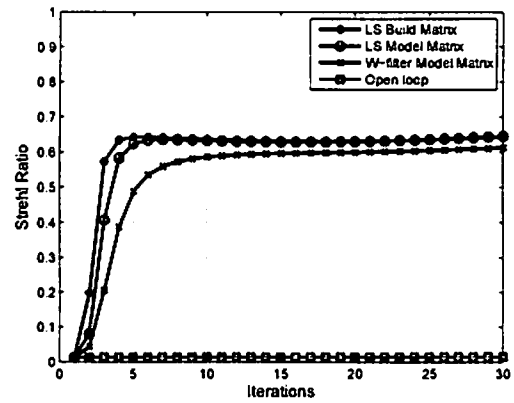

(c) Misregistration = 5%, $f_{3dB}/f_G = 15$

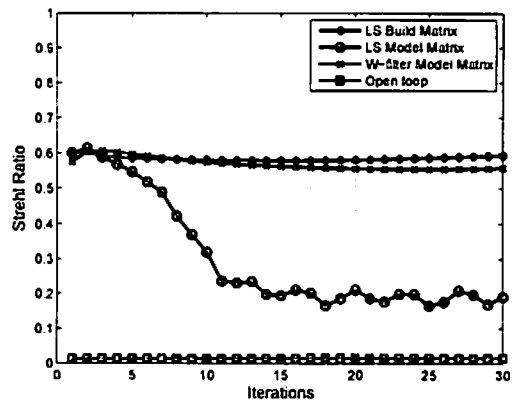

(d) Misregistration = 30%, $f_{3dB}/f_G = 15$

Figure 6. This figure gives the results of the 15 × 15 subaperture AO system using a SH WFS run over 30 iterations. Four different reconstruction matrices are used to calculate the four Strehl ratios on each plot. The four reconstruction matrices are the least-squares build, the least-squares model, the W-filter and open-loop. (a) Shows the matrix having a misregistration of 5% of a subaperture with a $f_{3dB}/f_G = 5$. (b) Shows the matrix having a misregistration of 30% of a subaperture with a $f_{3dB}/f_G = 5$. (c) Shows the matrix having a misregistration of 5% of a subaperture with a $f_{3dB}/f_G = 15$. (d) Shows the matrix having a misregistration of 30% of a subaperture with a $f_{3dB}/f_G = 15$.

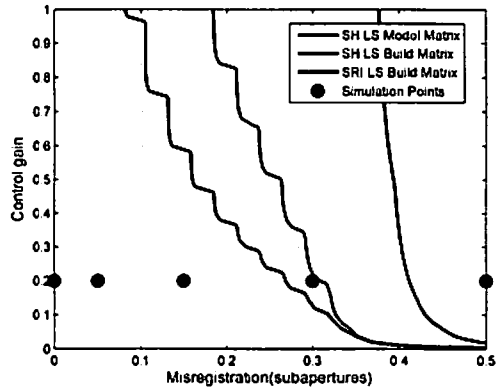

Figure 7. Stability lines of a 15 × 15 subaperture system. This figure illustrates the relationship of instability to misregistration and gain. The area under the curves is the stable region while the area above the curves is the unstable region. The least-squares model matrix refers to a WaveProp build reconstruction matrix, the least-squares build matrix refers to poke build SH reconstruction matrix, and the SRI least-squares build matrix refers to the SRI poke built SRI reconstruction matrix.

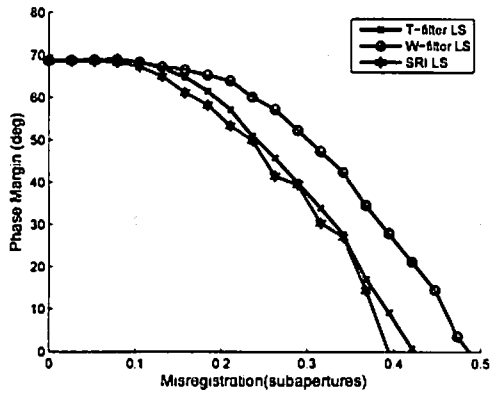

Figure 8. Phase margins of a 15 × 15 subaperture system. This figure illustrates the phase margins that were calculated for misregistration up to half of a subaperture. The build least squares reconstructor was evaluated as well as the T- and W- filters.

The final analytical calculation performed is displayed in Fig. 8. This graph shows that the measured reconstructor has similar phase margins as the T- and W-filters. The phase margins of each reconstruction matrix are not degraded much with misregistration until the misregistration reaches 20% of a subaperture.

4.2.2 Results

With the number of subapertures at 15 × 15, the model matrix begins to break down with higher misregistration. This is shown in Fig. 9 looking at plots (b) and (d); when the system has 30% misregistration, the model matrix has a strong downward slope. The geometry matrix and the W-filter are maintaining a steady Strehl ratio, especially in (d). Again, this is the point when the analytical calculations show that the system has reached a point of instability.

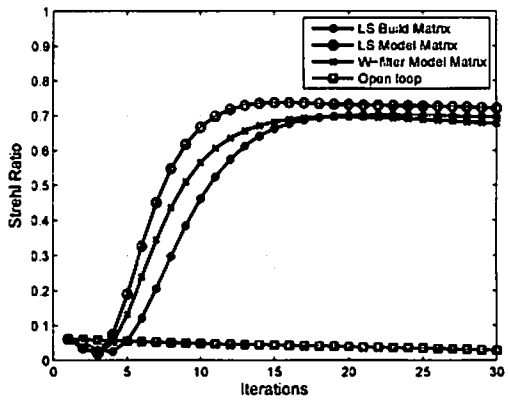

(a) Misregistration = 5%, $f_{3dB}/f_G = 5$

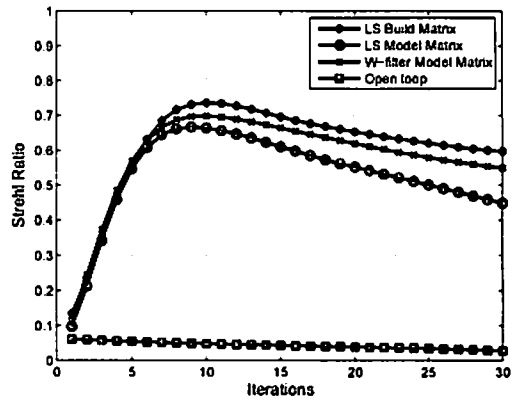

(b) Misregistration = 30%, $f_{3dB}/f_G = 5$

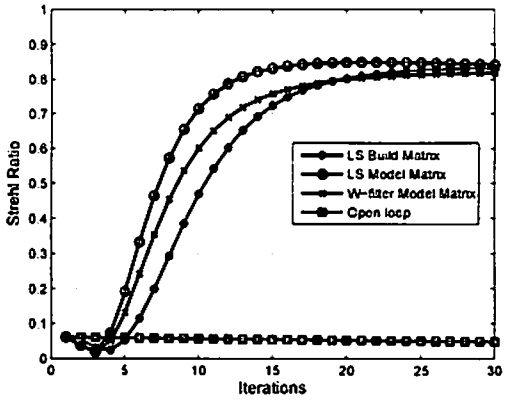

(c) Misregistration = 5%, $f_{3dB}/f_G = 15$

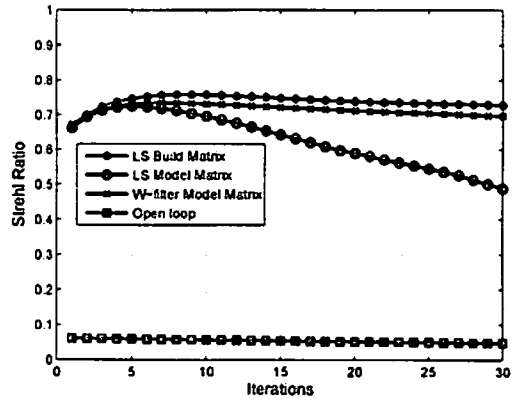

(d) Misregistration = 30%, $f_{3dB}/f_G = 15$

Figure 9. This figure gives the results of the 15 × 15 subaperture AO system using a SRI WFS run over 30 iterations. Four different reconstruction matrices are used to calculate the four Strehl ratios on each plot. The four reconstruction matrices are the least-squares build, the least-squares model, the W-filter and open-loop. (a) Shows the matrix having a misregistration of 5% of a subaperture with a $f_{3dB}/f_G = 5$. (b) Shows the matrix having a misregistration of 30% of a subaperture with a $f_{3dB}/f_G = 5$. (c) Shows the matrix having a misregistration of 5% of a subaperture with a $f_{3dB}/f_G = 15$. (d) Shows the matrix having a misregistration of 30% of a subaperture with a $f_{3dB}/f_G = 15$.

Table 2. SRI WFS Strehl ratio averages for a 15 × 15 subaperture system

f_{3dB}/f_G	Misregistration %	Build Matrix Strehl Ratio	Model Matrix Strehl Ratio	% Change
5	0%	0.67	0.77	-12.2 %
	5%	0.66	0.74	-10.8 %
	15%	0.61	0.69	-11.1 %
	30%	0.59	0.56	6.0 %
	50%	0.40	0.32	26.4 %
15	0%	0.75	0.87	-13.5 %
	5%	0.73	0.85	-13.1 %
	15%	0.64	0.79	-19.3 %
	30%	0.65	0.66	-1.5 %
	50%	0.45	0.41	10.6 %

5. SUMMARY

The purposes of this research were to study the effects of misregistration on AO systems and to analyze several means of mitigating it. Misregistration is a constant condition on all AO systems and is always a concern when setting up any experiment. Currently, this restriction requires highly trained engineers and very precise alignment procedures. However, in the field the AO system must be capable of performing at a high standard, and the time and talent to register the system to these exacting standards are not always available.

Specifically, this research studied how misregistration would affect a SH WFS differently than a SRI WFS. This research explored some of the differences between the reconstruction methods of a SH WFS and a SRI WFS. The same analysis was performed for each WFS, in order to estimate when each system would become unstable. Different mitigation strategies were examined, and a poke method was introduced. The mitigation strategy of using a unique reconstructor built using the WFS measurements was developed and tested for both the SH and SRI AO systems. The built reconstructor was compared against the model matrix used in most traditional AO settings. The simulations showed that for larger AO systems, the built matrix maintained the performance levels better than did the model matrix. Also, even with up to 50% misregistration, the built matrix showed much less system performance degradation than the model matrix.

5.1 Conclusions

It can be generally concluded that the introduction of the measured reconstruction matrix usually improved the systems' performance when there was a large amount of misregistration. Many things were learned from the result of this research. The main points taken from the research are that

- the measured matrix analytically shows a greater amount of resistance to instability due to misregistration,
- the poke matrix has a impact on the system to maintain stability and high performance when there is misregistration,
- the phase margin of the build SRI matrix predicted the higher resistance to instability with misregistration on the system,
- analytic calculations predict that the SRI WFS is less sensitive to misregistration than the SH WFS.

In summary, the design of a new reconstruction matrix using the measurements of the WFS was beneficial. This research shows the potential of correcting misregistration by constructing a unique poke matrix is a viable method. More work needs to be done to improve the performance of the system.

5.2 Recommendations

This research was limited in its scope to two very simple cases to keep the study focused on reconstruction. The next step would be to simulate a real-world AO system with noise, slaves, and a circular aperture. Another direction this research could take would be to study the combination of mitigation strategies. The use of the W-filter showed very solid results, so the combination of the build matrix and W-filter has strong possibilities of improving performance and stability. The phase margins and stability of the simulation could be analyzed to gain a more direct comparison with the analytic calculations. Finally, the process should be tested on a real AO system so it could be studied experimentally.

REFERENCES

[1] Tyson, R. K., [*Introduction to Adaptive Optics*], SPIE Press (2000).

[2] Andrews, L. C. and Phillips, R. L., [*Laser Beam Propagation through Random Media*], SPIE Press, 2nd ed. (2005).

[3] Brennan, T. J., "Hartmann sensor misregistration: Stability and stability margins," Tech. Rep. 1426, The Optical Sciences Company (August 1998).

[4] Rhoadarmer, T. A., "Development of a self-referencing interferometer wavefront sensor," *SPIE* **5553** (2004).

[5] Brennan, T. J., "The use of spatial filtering techniques to reduce ABL stability margin loss," Tech. Rep. 1450, the Optical Sciences Company (April 1999).

DISTRIBUTION LIST

DTIC/OCP
8725 John J. Kingman Rd, Suite 0944
Ft Belvoir, VA 22060-6218 1 cy

AFRL/RVIL
Kirtland AFB, NM 87117-5776 2 cy

Nathan Engstrom
Official Record Copy
AFRL/RDSA 1 cy